DATA REPOSITORY ITEM 2006068

APPENDIX 1. ANALYTICAL METHODS

U-Pb isotopic measurements were made mainly on single zircons separated from the rock samples using standard techniques. Minerals were analysed by ID-TIMS methods (Parrish and Noble, 2003) using a ^{205}Pb–^{233}U–^{235}U tracer and two mass spectrometers (a ThermoElemental Triton and a VG354) using single Re filaments and arrays of both faraday and ion counting detectors. Chemical and mass spectrometric methods were similar to Parrish et al. (1987) and Noble et al. (1993). A solution made from the zircon standard 91500 was measured together with several U and Pb blanks which averaged <0.4pg and <5pg, respectively. Decay constants for ^{238}U and ^{235}U used are those recommended by Steiger and Jäger (1977).

Hf isotope ratios were measured on a ThermoElemental Axiom MC-ICP-MS at the NERC Isotope Geosciences Laboratory. Zr-Hf solutions were saved from the U-Pb column washes of dissolved, abraded single zircons, dried down and converted to weak HNO_3-HF solutions, which were then aspirated directly into the plasma. Solutions were unspiked, and $^{176}Lu/^{177}Hf$ ratios were determined using the isobar-free ^{175}Lu peak and were normalised to those measured for the 91500 zircon according to the recommended value of Wiedenbeck et al. (1995). Corrections were made to Hf isotopes for Lu and Yb isobars using the procedure of Nowell and Parrish (2001). The series of measurements was divided into ten sessions over a six week period in which sample measurements could be bracketed by standards measured under relatively uniform instrumental operating conditions. The average of standard measurements obtained during each of these periods was used to normalize sample results relative to an assumed $^{176}Hf/^{177}Hf$

value of 0.282160 for JMC475. Seventy-nine determinations of JMC475 (including those doped with Lu and Yb) yielded a mean of 0.282151 ± 0.000014 (2σ). The average $^{176}Hf/^{177}Hf$ value of the 27 measurements of the 91500 zircon standard is 0.282298 ± 20 (2σ), after normalization to the JMC475 standard measurements run during the same analytical session. The values measured by Wiedenbeck et al. (1995) and Amelin et al. (2000) were 0.282302 ± 8 and 0.282317 ± 28, respectively, after normalization to the same value of JMC475 used here. The average $^{178}Hf/^{177}Hf$ for all samples is 1.467197 ± 62 (2σ), whilst that for all 91500 zircon analyses is 1.467204 ± 66 (2σ). Normalisation has not been applied to these stable isotope ratios. Previous Hf isotopic studies have shown that Zr-Hf washes from the U-Pb columns may preserve the true Lu/Hf ratios of the samples (Amelin et al., 1999). For example, during this study the difference between true and measured Lu/Hf of the 91500 zircon solution was only 0.17%. The major correction to the ^{176}Hf peak was for ^{176}Yb, which was monitored using ^{173}Yb. Combined internal and external errors are quoted at the 2σ level. Although internal errors are about ±0.2ε unit for all but the smallest samples, day-to-day variations of the JMC475 standard limit the external reproducibility to about ± 1ε unit.

A major problem in evaluating $T_{DM}Hf$ or ε_{Hf} is choosing the correct value for the ^{176}Lu decay constant, which is not precisely resolved (Davis et al., 2005). For this study, we have used 1.94 x 10^{-5}/m.y. The Lu-Hf ratio in zircon is highly fractionated relative to the magma from which it crystallized. Therefore, calculation of Hf model ages in zircon is subject to interpretation, in contrast to whole-rock model Nd ages. Model ages must be determined by using an inferred Lu/Hf value for 'source' rocks prior to zircon crystallization, making the calculation a two-stage process. In the present case we use a

$^{176}Lu/^{177}Hf$ value of 0.012, broadly consistent with the range of Lu/Hf ratios measured in crustal rocks of the Superior province (range: 0.012–0.015; Stevenson and Patchett, 1990) and with Precambrian granitoid rocks (0.0093; Vervoort and Patchett, 1996). Model age and epsilon calculations also depend on the parameters chosen to define the depleted mantle and chondritic growth curve, and in this study we use 0.282772 and 0.0332, and 0.28325 and 0.0384 (Blichert-Toft and Albarède, 1997) for $^{176}Hf/^{177}Hf$ and $^{176}Lu/^{177}Hf$ ratios of chondritic and depleted mantle reservoirs, respectively.

Nd isotope ratios were collected on a Triton thermal ionization mass spectrometer at the Department of Earth Sciences, The Open University. Standard sample preparation and isotopic analytical techniques are described in Cohen et al. (1988). $^{143}Nd/^{144}Nd$ ratios were normalised to $^{146}Nd/^{144}Nd = 0.7219$. Repeat analyses of the Johnson-Matthey internal standard gave 0.511816 ± 6 (2σ) for a 3 month period during the period of sample analysis, corresponding to a value of BHVO-2 (external standard) of 0.512976 ± 14. Total procedural Nd blanks were < 1 ng. $^{147}Sm/^{144}Nd$ ratios were calculated from elemental ratios obtained from quadrupole ICP-MS. The Sm-Nd model ages given in Table DR-3 are calculated relative to a depleted mantle from the quadratic solution using the parameters of DePaolo et al. (1981).

APPENDIX 2. ZIRCON DESCRIPTIONS

Two zircon populations were observed from a massive, recrystallised quartzite of the Daling-Shumar group (B75), within a well-layered section. The first comprises colourless, prismatic, subhedral crystals, most of which are rich in inclusions, while the

second population comprsises well-rounded, anhedral, inclusion-free crystals. Moderate U concentrations of 40–420 ppm were recorded.

A quartz-sericite meta-rhyolite also from the Daling-Shumar Group from higher in the stratigraphic section (RP109) yielded well-developed prismatic zircons that are pink to clear; some appear turbid, broken or cracked. Imaging these zircons reveals core-rim morphology, suggesting an inherited core with a magmatic rim indicative of crystallisation. U concentrations in abraded grains have a moderate spread of ~300–500 ppm U. Monazites have diverse U contents, 240–7000 ppm U, and reflect original magmatic grains and later metamorphic overgrowths.

The High Himalayan Series metaquartzite (RP71) from the footwall of the Kakhtang thrust contains zircon morphologies that display equant to elongate morphologies with some evidence of sedimentary abrasion. Moderate variations of U concentrations of ~240–660 ppm U were measured.

Heavy minerals recovered from an augengneiss intruding metasediments in the hanging wall of the Kakhtang thrust (RP69) included both monazite (igneous and metamorphic) and igneous zircon crystals. Variations in U from subhedral zircons ranged from ~400–700 ppm. Seven single grain monazite fractions yielded U concentrations between ~2000–7500 ppm, with huge variations in model Th/U ratio, with highest Th/U intrinsic to the relic magmatic components, and the lower Th/U in the much younger metamorphic component.

APPENDIX 3. U-Pb ISOTOPE RESULTS

A massive quartzite was collected as a representative sample of the Daling-Shumar Formation. Single zircon analyses from this quartzite (B75) yielded two $^{207}Pb/^{206}Pb$ age groups (Fig. 3a): 1.85 to 2.00 Ga (n=12) and 2.45 to 2.55 Ga (n=2).

Single and multigrain zircons from a meta-rhyolite within the Daling-Shumar Group (RP109) consisted of igneous and inherited composite grains yielding $^{207}Pb/^{206}Pb$ ages ranging from 1.79–1.89 Ga. The scatter in zircon data is due mainly to zircon inheritance with modest Pb loss. Two analyses of homogeneous monazite are concordant at 18–20 Ma while all four monazite analyses define a discordia line between 20 Ma and 1.76 ± 0.15 Ga (95% confidence). If the youngest zircon (Z5) is regressed with the monazites, the upper intercept is 1785 ± 34 Ma, a reasonable, but maximum age for igneous crystallization (since Z5 may have contained a very small older core). Deposition of the quartzite is thus dated at 1.75 Ga or earlier.

Nine single-grain zircons from a High Himalayan Series metaquartzite (RP71) from the footwall of the Kakhtang thrust yielded $^{207}Pb/^{206}Pb$ ages from 0.98–1.82 Ga, (Fig. 3a).

Four zircon and seven monazite fractions (mostly single grain) from an augen orthogneiss intruding metasediments in the hanging wall of the Kakhtang thrust (RP69) were dated. Four monazites have a weighted mean $^{207}Pb/^{235}U$ age of 14.30 ± 0.35 Ma and together with three other monazites define a chord with upper intercept of 812 ± 20 Ma (MSWD = 7.8). The three most discordant zircons are co-linear with an upper intercept 832 ± 6 Ma (MSWD = 0.4) while the fourth zircon has a slightly older $^{207}Pb/^{206}Pb$ age of 847 Ma, suggesting minor inheritance that was not clearly visible. If the three co-linear zircons

and all monazites are regressed together, the upper intercept is 825 ± 9 Ma (MSWD = 8.3) which we take as the best estimate of crystallization age of the augengneiss.

Additional references

Blichert-Toft, J., and Albarède, F., 1997, The Lu-Hf isotope geochemistry of chondrites and the evolution of the crust-mantle system: Earth and Planetary Science Letters, v. 148, p. 243–258.

Cohen, A.S., Onions, R.K., Siegenthaler, R., and Griffin, W.L., 1988, Chronology of the pressure-temperature history recorded by a granulite terrain: Contributions to Mineralogy and Petrology, v. 98, p. 303–311.

Davis, D.W., Amelin, Y., Nowell, G., and Parrish, R.R., 2005, Hf isotopes in zircon from the western Superior province, Canada: Implications for Archean crustal development and evolution of the depleted mantle reservoir: Precambrian Research, v. 140, p. 132-156.

DePaolo, D.J., 1981, Neodymium isotopes in the Colorado Front Range and implications for crust formation and mantle evolution in the Proterozoic: Nature, v. 291, p. 193–197.

Noble, S.R., Tucker, T.C., and Pharaoh, T.C., 1993, Lower Palaeozoic and Precambrian igneous rocks from eastern England, and their bearing on late Ordovician closure of the Tornquist Sea: Constraints from U-Pb and Nd isotopes: Geological Magazine, v. 130, p. 835–846.

Nowell, G., and Parrish, R.R., 2001, Simultaneous acquisition of isotope compositions and parent/daughter ratios by non-isotope dilution-mode Plasma Ionisation Multi-collector Mass Spectrometry (PIMMS), in Holland, G., and Tanner, S. D., eds., Plasma source mass spectrometry: The new millenium, Proceedings of the 7th

International Conference on Plasma Source Mass Spectrometry, Royal Society of Chemistry, p. 298–310.

Parrish, R.R., Roddick, J.C., Loveridge, W.D., and Sullivan, R.W., 1987, Uranium-lead analytical techniques at the geochronology laboratory: Geological Survey of Canada Paper, v. 87–2, p. 3–7.

Parrish, R.R., and Noble, S.R., 2003, Zircon U-Pb geochronology by isotope dilution – thermal ionisation mass spectrometry (ID-TIMS), in Hanchar, J.M., and Hoskin, P.W.O., eds., Zircon: Reviews in Mineralogy and Geochemistry, Mineralogical Society of America and Geochemical Society, p. 183–213.

Steiger, R.H., and Jäger, E., 1977, Subcommission on Geochronology: Convention on the use of decay constants in geo- and cosmochronology: Earth and Planetary Science Letters, v. 36, p. 359–362.

Vervoort, J.D., and Patchett, P.J., 1996, Behavior of hafnium and neodymium isotopes in the crust: Constraints from Precambrian crustally derived granites: Geochimica et Cosmochimica Acta, v. 60, p. 3717–3733

Wiedenbeck, M., Allé, P., Corfu, F., Griffin, W.L., Meier, M., Oberli, F., Von Quadt, A., Roddick, J.C., and Spiegel, W., 1995, Three natural zircon standards for U-Th-Pb, Lu-Hf, trace element and REE analysis: Geostandards Newsletter, v. 19, p. 1–23.

TABLE DR-1. U-Pb ISOTOPIC DATA

Analysis[a]	Weight (mg)	U (ppm)	Pb (ppm)	Pbc (pg)[b]	$^{206}Pb/^{204}Pb$[c]	Th/U[d]	$^{206}Pb/^{238}U$[e]	± 1 std err (%)	$^{207}Pb/^{235}U$[e]	± 1 std err (%)	$^{207}Pb/^{206}Pb$[e]	± 1 std err (%)	$^{206}Pb/^{238}U$[e] (Ma)	± 2 std err (Ma)	$^{207}Pb/^{235}U$[e] (Ma)	± 2 std err (Ma)	$^{207}Pb/^{206}Pb$[e] (Ma)	± 2 std err (Ma)	Correlation coefficient	% discordance[f]
RP69 - Augengneiss, Takhtsang Formation above Kakhtang thrust																				
Z1 (U,L,1)	0.0094	689.9	86.10	21	2517	0.23	0.1276	0.14	1.184	0.18	0.06730	0.10	774.1	2.1	793.1	2.0	847.1	4.1	0.84	9
Z2 (U,L,1)	0.0092	560.1	66.87	19	2085	0.24	0.1218	0.17	1.120	0.20	0.06673	0.12	740.8	2.3	763.2	2.1	829.3	4.8	0.81	11
Z3 (U, 2)	0.0036	548.8	48.08	14	813	0.24	0.08925	0.30	0.817	0.39	0.06641	0.22	551.1	3.2	606.5	3.5	819.4	9.3	0.82	34
Z5 (U, 3)	0.0085	394.2	47.73	82	2998	0.42	0.1177	0.16	1.082	0.19	0.06664	0.10	717.4	2.3	744.4	2.0	826.6	4.1	0.85	14
M1 (A,1)	0.0044	2020	1788	10	2897	59.9	0.05110	0.54	0.4610	0.56	0.06543	0.20	321.3	3.4	385.0	3.6	788.3	8.5	0.93	61
M2 (A,1)	0.0013	7479	56.34	5	266	9.22	0.002173	0.81	0.01333	2.69	0.04447	2.50	14.00	0.23	13.44	0.72	-84	122	0.38	RD
M3 (A,1)	0.0560	2697	1111	66	4789	41.2	0.03356	1.22	0.3031	1.26	0.06552	0.15	212.8	5.1	268.8	6.0	790.9	6.4	0.99	74
M4 (A,2)	0.0025	7010	51.67	5	532	8.66	0.002227	0.28	0.01420	0.62	0.04627	0.50	14.34	0.08	14.32	0.18	11.5	24.1	0.60	RD
M5 (1)	0.0046	7491	326.4	7	1449	31.5	0.004510	0.25	0.03461	0.32	0.05566	0.21	29.01	0.15	34.55	0.22	438.9	9.5	0.74	94
M6 (3)	0.0220	6460	51.55	27	754	9.30	0.002288	0.99	0.01448	1.03	0.04590	0.24	14.73	0.29	14.60	0.30	-7.5	11.4	0.97	RD
M7 (1)	0.0086	6576	47.91	20	402	8.45	0.002241	0.24	0.01412	0.63	0.04569	0.53	14.43	0.07	14.23	0.18	-18.7	25.7	0.57	RD
RP71 - Quartzite, High Himalayan metasediment, below Kakhtang thrust																				
Z1 (D,U,1)	0.0020	662.6	112.8	20	671	0.61	0.1570	0.43	1.571	0.50	0.07254	0.30	940.2	7.6	958.7	6.2	1001	12	0.80	7
Z2 (D,U,1)	0.0018	327.0	53.61	5	1211	0.32	0.1630	0.23	1.612	0.31	0.07170	0.20	974.0	4.0	975.0	4.0	978.0	8.0	0.70	1
Z3 (D,E,1)	0.0046	415.8	121.6	4	8463	0.20	0.2905	0.33	4.467	0.33	0.11150	0.06	1644	10	1725	6	1824	2	0.98	11
Z4(D,O,1)	0.0030	532.1	96.3	17	1011	0.45	0.1736	0.22	1.816	0.28	0.07586	0.16	1032	4	1051	4	1091	7	0.82	6
Z5 (D,L,1)	0.0041	399.0	73.62	8	2255	0.70	0.1655	0.19	1.899	0.23	0.08324	0.14	987.1	3.4	1081	3	1275	5	0.81	24
Z6 (D,O,1)	0.0058	587.8	136.4	120	399	0.49	0.2183	0.24	2.585	0.44	0.08588	0.32	1273	6	1297	7	1336	12	0.71	5
Z7 (D,E,1)	0.0029	247.4	52.55	12	753	0.54	0.1970	0.21	2.545	0.25	0.09372	0.13	1159	4	1285	4	1502	5	0.86	25
Z8 (D,O,1)	0.0018	451.0	120.9	14	897	0.57	0.2462	0.23	3.321	0.26	0.09782	0.14	1419	6	1486	4	1583	5	0.84	12
Z9 (D,O,1)	0.0025	241.8	66.22	7	1377	0.69	0.2444	0.22	3.287	0.25	0.09754	0.12	1410	6	1478	4	1578	4	0.89	12
B75z - Quartzite, Daling-Shumar Group																				
Z1 (D,A,E,CL,	0.0067	94.77	36.21	50	284	0.60	0.3428	0.19	5.755	0.43	0.1218	0.34	1900	6	1940	7	1982	12	0.66	5
Z2 (D,A,E,1)	0.0044	160.3	85.80	375	71	0.64	0.4602	2.18	10.707	2.90	0.1687	1.10	2441	89	2498	39	2545	40	0.84	5
Z3 (D,A,L,1)	0.0107	202.7	75.50	50	942	0.46	0.3456	0.17	5.719	0.21	0.1200	0.11	1914	6	1934	4	1956	4	0.85	3
Z4 (D,A,E,CL,	0.0042	41.37	15.18	43	854	0.53	0.3354	0.12	5.494	0.19	0.1188	0.11	1865	4	1900	3	1938	4	0.80	4
Z5 (D,A,E,1)	0.0045	307.6	110.8	56	557	0.21	0.3539	0.21	6.001	0.29	0.1230	0.17	1953	7	1976	5	2000	6	0.81	3
Z6 (D,A,E,1)	0.0050	328.6	105.1	48	697	0.20	0.3176	0.12	4.995	0.22	0.1141	0.15	1778	4	1819	4	1865	5	0.76	5
Z8 (D,CL,A,E,	0.0039	209.2	77.26	12	1422	0.50	0.3395	0.15	5.575	0.18	0.1191	0.08	1884	5	1912	3	1943	3	0.89	4
Z9 (D,A,E,1)	0.0037	188.6	97.82	7	2764	0.69	0.4452	0.13	9.784	0.14	0.1594	0.06	2374	5	2415	3	2449	2	0.89	4
Z10 (D,A,E,1)	0.0038	140.7	51.28	5	2281	0.51	0.3351	0.17	5.452	0.18	0.1180	0.10	1863	5	1893	3	1926	4	0.84	4
Z11 (D,A,E,1)	0.0048	423.0	139.8	61	699	0.14	0.3308	1.06	5.537	1.08	0.1214	0.21	1842	34	1906	19	1977	8	0.98	8
Z12 (D,A,E,1)	0.0046	391.0	129.2	9	4203	0.27	0.3210	0.11	5.175	0.12	0.1169	0.05	1795	4	1849	2	1910	2	0.93	7
Z13 (D,A,L,1)	0.0048	181.4	63.26	10	1718	0.42	0.3279	0.51	5.132	0.51	0.1135	0.09	1828	16	1841	9	1856	3	0.98	2
Z14 (D,A,E,1)	0.0041	114.2	39.87	9	1073	0.50	0.3226	0.15	5.042	0.18	0.1134	0.10	1802	5	1826	3	1854	4	0.81	3
Z15 (D,A,L,1)	0.0037	209.7	72.56	9	1715	0.51	0.3183	0.11	5.067	0.13	0.1154	0.08	1782	3	1831	2	1887	3	0.80	6
RP109 - Metarhyolite, Daling-Shumar Group																				
Z1 (U,2)	0.0122	479.1	133.6	21	4656	0.29	0.2701	0.933	4.306	0.95	0.1156	0.15	1541	26	1694	16	1889	5	0.98	21
Z2 (U,3)	0.0107	363.4	114.7	42	1709	0.43	0.2965	0.25	4.548	0.26	0.1112	0.072	1674	7	1740	4	1820	2.6	0.96	9
Z3 (U,3)	0.0113	342.3	116.0	6	13430	0.33	0.3263	0.13	5.066	0.14	0.1126	0.044	1821	4.1	1831	2	1842	2	0.95	1
Z4 (U,1)	0.0015	320.5	101.0	5	1755	0.27	0.3083	0.23	4.667	0.24	0.1098	0.11	1732	7	1761	4	1796	4	0.90	4
Z5 (U,1)	0.0018	305.9	95.53	5	2148	0.16	0.3139	0.19	4.731	0.2	0.1093	0.091	1760	6	1773	3	1788	3	0.89	2
Z26 (U,1)	0.0016	294.8	95.94	20	488	0.25	0.3192	0.85	4.918	1.21	0.1117	0.94	1786	26	1805	20	1828	33	0.64	3
Z27 (U,12)	0.0388	493.9	143.4	23	14800	0.25	0.2847	0.14	4.364	0.15	0.1112	0.04	1615	4	1706	3	1819	1	0.97	13
M1 (A,1)	0.0269	5160	64.31	84	341	11.1	0.003134	0.23	0.01991	0.62	0.04608	0.5	20.17	0.09	20.02	0.24	2	24	0.65	RD
M2 (U,1)	0.0025	7332	78.36	61	70	10.5	0.002794	0.83	0.01880	3.3	0.04881	2.8	17.99	0.30	18.92	1.24	139	132	0.67	0
M3 (L,1)	0.0005	1680	718.3	7	790	11.8	0.1035	0.29	1.508	0.42	0.1057	0.29	634.7	3.5	933.4	5.1	1726	11	0.72	66
M4 (A,1)	0.0018	240.2	93.42	4	245	34.7	0.03704	0.43	0.5424	0.82	0.1062	0.65	234.5	2.0	440.0	5.8	1735	24	0.61	88

[a], Z, zircon; M, monazite; Number of grains shown in parentheses. D, detrital; T, magmatic; U, euhedral, A, anhedral; E, equant; L, elongate; O, oval; CR, cracks; CL, clear

[b] Total common Pb in analysis, corrected for spike and Pb fractionation.

[c] Corrected for spike contribution and fractionation

[d] Atomic ratio of Th to U, calculated from radiogenic $^{208}Pb/^{206}Pb$.

[e] Corrected for blank Pb and U, and common Pb (Stacy-Kramers model Pb equivalent to interpreted age of mineral)

[f] RD, reverse discordance

TABLE DR-2. Lu-Hf ISOTOPIC DATA

	Sample[a]	$^{176}Hf/^{177}Hf$[b]	± 1σ abs	$^{76}Lu/^{177}Hf$	± 1σ abs	U-Pb age[c] (Ma)	± 2σ	$^{76}Hf/^{177}Hf_i$	$\varepsilon_{Hf}(T)$ [d]	± 2σ	T_{DM} Hf [d] (Ma)	± 2σ
B75z	Z1	0.281572	0.000006	0.000786	0.000080	1982	12	0.281541	2.5	1.2	2378	27
	Z2	0.281279	0.000010	0.000675	0.000068	2545	40	0.281245	5.4	2.8	2666	36
	Z3	0.281641	0.000006	0.001300	0.000132	1956	4	0.281591	3.6	0.9	2295	31
	Z4	0.281491	0.000007	0.000706	0.000072	1938	4	0.281464	-1.3	0.9	2549	30
	Z5	0.281664	0.000007	0.000563	0.000057	2000	6	0.281642	6.5	0.9	2173	25
	Z6	0.281515	0.000007	0.000836	0.000085	1865	5	0.281484	-2.3	0.9	2545	30
	Z7	0.281635	0.000007	0.000632	0.000064	1865[e]		0.281612	2.2	0.9	2299	27
	Z8	0.281553	0.000008	0.000300	0.000030	1943	3	0.281541	1.6	0.8	2397	25
	Z9	0.281192	0.000008	0.001005	0.000102	2449	2	0.281143	-0.5	1.0	2913	38
	Z10	0.281546	0.000008	0.000545	0.000055	1926	4	0.281526	0.6	0.9	2436	29
	Z12	0.281502	0.000007	0.000320	0.000032	1910	2	0.281490	-1.0	0.7	2513	25
	Z13	0.281572	0.000008	0.000459	0.000047	1856	3	0.281555	0.0	0.8	2414	28
	Z14	0.281512	0.000008	0.000268	0.000027	1854	4	0.281502	-1.9	0.8	2517	26
	Z15	0.281545	0.000009	0.000557	0.000056	1887	3	0.281525	-0.3	0.9	2457	32
RP109	Z26	0.281581	0.000005	0.001192	0.000121	1827	34	0.281538	-1.2	1.8	2459	31
	Z27	0.281496	0.000012	0.001351	0.000137	1819	3	0.281447	-4.7	1.3	2639	54

[a] All single grains except Z27 (multi-grain)

[b] corrected for Lu and Yb interference and normalised to 0.282160 for JMC 475 Hf; Lu/Hf normalised to 0.000288 for the 91500 zircon

[c] interpreted age of zircon from radiogenic $^{207}Pb/^{206}Pb$

[d] decay constant used for ^{176}Lu: $1.94e^{-11}$/year; chondritic and DM Lu/Hf and $^{176}Hf/^{177}Hf$: 0.332, 0.282772 and 0.0384, 0.28325;
DM age calculated in two stages (see text for more details)

[e] U-Pb age for this zircon failed; an age of 1865 Ma is assumed to calculate parameters

TABLE DR-3. MAJOR, TRACE AND Nd, Sr DATA FOR METASEDIMENTARY FORMATIONS

	HHS (N. of Kakhtang thrust)			HHS (S. of Kakhtang thrust)													Daling-Shumar Formation (LHS)				
Sample	**B45**	**B87**	**Bh3**	**B39**	**B41**	**B50**	**B51**	**B68**	**B71b**	**B81**	**B83**	**B85[b]**	**B88[b]**	**Bh6**	**Bh10[b]**	**Bh12**	**B29a**	**B29b**	**B36a**	**B75**	**Bh13**
Rock type	Bt gneiss	Bt gneiss	Bt-sill gneiss	Ky schist	Bt gneiss	Sill schist	Mica schist	Bt gneiss	Quartzite	Gnt phyllite	Gnt schist	Gnt schist	Gnt schist	Bt gneiss	Gnt schist	Gnt schist	Quartzite	Phyllite	Phyllite	Quartzite	Phyllite
Latitude (N)	27° 35.03'	27° 29.83'	27° 51.97'	27° 20.31'	27° 25.93'	27° 20.84'	27° 20.82'	27° 14.21'	27° 17.89'	27° 27.41	27° 30.91'	27° 23.40'	27° 18.88'	27° 37.76	27° 18.89'	26° 55.05'	27° 16.32'	27° 16.32'	27° 15.91'	27° 16.10'	26° 54.07'
Longditude (E	91° 29.89'	89° 21.25'	89° 43.55'	91° 32.76'	91° 34.18'	91° 37.08'	91° 37.62'	91° 33.12'	91° 28.48'	90° 22.07'	90° 17.74'	89° 35.24'	89° 32.92'	89° 49.23'	89° 32.74'	89° 28.45'	91° 14.87'	91° 14.87'	91° 23.82'	91° 23.74'	89° 27.00'
Wt %																					
SiO_2	75.75	69.25		63.99	70.50	74.69	84.05	74.23	95.79	69.11	58.04	71.93	65.55				93.15	68.20	76.93	97.89	
TiO_2	0.30	0.78		0.92	0.52	0.79	0.59	0.29	0.12	0.77	1.05	0.73	0.77				0.22	0.59	0.94	0.08	
Al_2O_3	13.10	15.99		19.83	14.19	12.63	7.91	13.42	3.47	17.75	19.88	13.97	17.30				3.25	16.18	11.49	2.62	
Fe_2O_3[a]	2.26	6.53		7.94	3.31	4.97	3.53	2.43	1.30	5.61	11.40	6.37	6.35				0.44	4.67	2.64	0.63	
MnO	0.03	0.08		0.17	0.04	0.10	0.07	0.04	0.03	0.12	0.21	0.05	0.08				0.00	0.02	0.01	0.01	
MgO	1.20	1.72		1.77	1.72	1.65	0.99	0.96	0.34	1.22	1.97	1.95	1.58				0.45	1.73	1.91	0.53	
CaO	1.73	0.79		0.33	1.92	0.36	0.24	1.10	0.02	0.24	1.15	0.96	0.96				0.04	0.09	0.12	0.04	
Na_2O	3.42	1.75		0.45	2.67	0.34	0.27	2.97	0.02	0.71	1.56	1.04	2.57				0.01	0.16	0.11	0.01	
K_2O	2.12	3.92		3.93	3.81	3.12	1.97	3.78	2.01	4.34	4.18	3.51	3.00				1.23	5.28	4.08	0.79	
P_2O_5	0.16	0.09		0.05	0.14	0.22	0.17	0.13	0.03	0.06	0.29	0.11	0.07				0.02	0.08	0.10	0.03	
LOI	0.59	0.67		1.47	0.96	1.62	1.16	0.82	0.41	2.10	2.64	1.64	1.61				0.71	2.63	1.93	0.52	
Total	100.65	101.57		100.84	99.78	100.50	100.95	100.17	103.54	102.03	102.37	102.27	99.82				99.52	99.63	100.27	103.16	
ppm																					
Rb	133	164	77	227	182	163	92	166	77	283	247	144	163	268	114	153	198	42	220	33	232
Sr	123	182	60	37	118	45	15	102	17	38	166	40	157	69	140	159	53	10	43	4	82
Ba	231	882		662	572	706	260	541	230	712	642	794	549				777	304	682	76	
Y	19	32		37	27	35	26	35	10	35	50	35	35				23	6	45	5	
Zr	108	230		239	142	272	250	128	67	238	210	332	208				232	609	809	113	
Nb	11	15		20	14	14	11	13	3	17	22	15	16				14	5	22	2	
Th	14	13		21	14	19	10	17	5	17	27	21	14				16	6	78	4	
U	4	3		3	3	4	4	3	2	15	6	5	2				4	3	14	1	
Nd	28.02	45.81	23.11	45.69	50.69	37.90	30.25	31.60	11.78	47.12	67.70	41.68	40.42	19.00	30.65	32.18	6.23	31.93	74.28	9.21	49.24
Sm	5.85	8.84	4.75	9.08	10.15	7.74	6.10	6.69	2.39	9.65	13.77	8.24	8.21	3.94	6.34	6.61	1.05	5.68	13.09	1.68	7.54
$^{87}Rb/^{86}Sr$	3.13	2.61		17.68	4.47	10.46	17.80	4.71	13.08	21.40	4.31	10.32	3.01				10.87	12.07	14.92	24.85	
$^{87}Sr/^{86}Sr$	0.75348	0.74394		0.83617	0.77531	0.77506	0.83681	0.76448	0.92056	0.80052	0.72775	0.78961	0.75981				0.91818	0.88034	0.97145	1.05902	
Error (± 2σ)	0.00002	0.00001		0.00002	0.00003	0.00002	0.00001	0.00002	0.00002	0.00001	0.00001	0.00002	0.00001				0.00002	0.00001	0.00002	0.00004	
$^{147}Sm/^{144}Nd$	0.126	0.117	0.124	0.120	0.121	0.124	0.122	0.128	0.122	0.124	0.123	0.119	0.123	0.125	0.122	0.124	0.102	0.107	0.106	0.110	0.092
$^{143}Nd/^{144}Nd$	0.511884	0.511780	0.512015	0.511795	0.511867	0.511873	0.511803	0.511877	0.511738	0.511932	0.512017	0.511801	0.511908	0.511875	0.511773	0.511789	0.511253	0.511274	0.511238	0.511312	0.510984
Error (± 2σ)	0.000006	0.000023	0.000003	0.000009	0.000005	0.000008	0.000006	0.000007	0.000002	0.000003	0.000004	0.000006	0.000011	0.000002	0.000003	0.000003	0.000008	0.000005	0.000008	0.000007	0.000001
$\varepsilon_{Nd}(500)$	-10.2	-11.6	-7.5	-11.6	-10.2	-10.3	-11.5	-10.5	-12.8	-9.1	-7.4	-11.4	-9.5	-10.3	-12.1	-11.9	-21.0	-20.9	-21.6	-20.4	-25.6
T(DM) (Ga)	2.03	2.00	1.75	2.05	1.95	1.99	2.07	2.09	2.20	1.89	1.73	2.02	1.91	2.02	2.14	2.14	2.46	2.57	2.60	2.58	2.61

[a] All Fe calculated as Fe_2O_3 [b] Identified as Jaishidamda Formation (Daniel et al., 2003)

Figure DR-1 (a) Concordia diagram of young monazites from sample RP69.

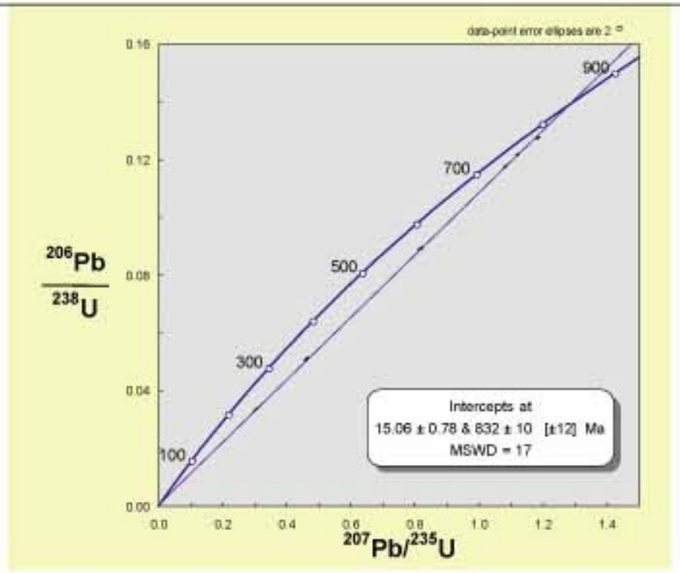

Figure DR-1 (b) Concordia diagram of all monazite and zircon data with a regression line shown only for reference.

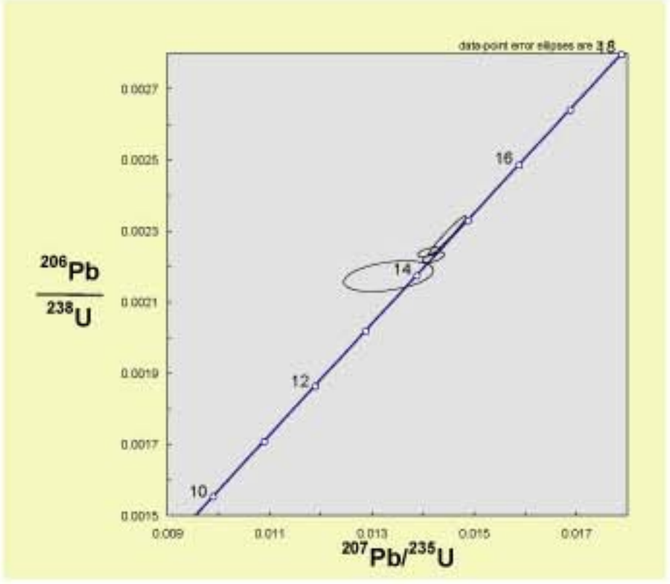

Figure DR-1 (c) Concordia diagram for all single detrital zircons from sample RP71.

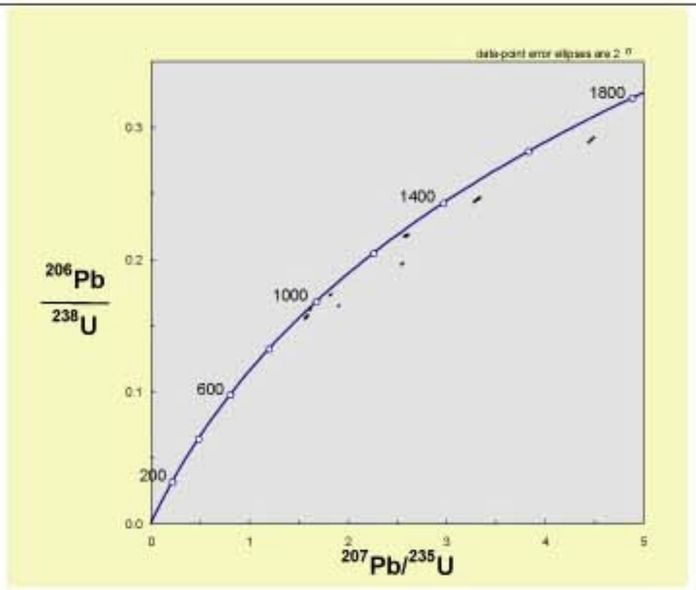

Figure DR-1 (d) Concordia diagram for all detrital zircons from sample B75.

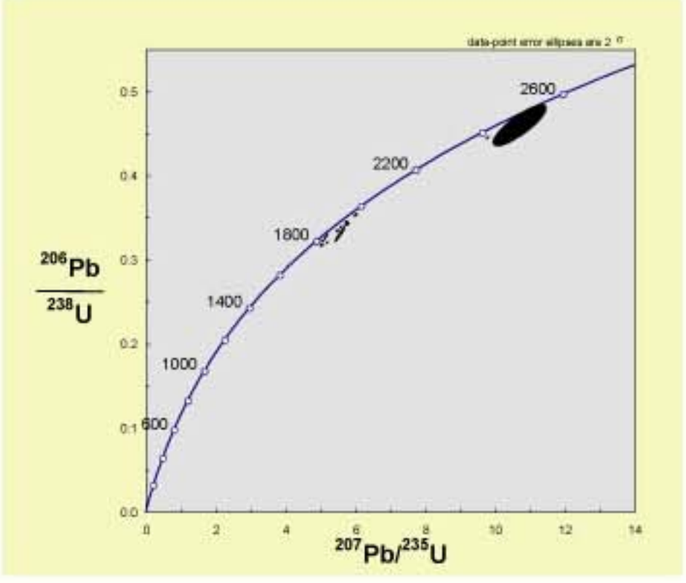

Figure DR-1 (e) Concordia diagram of all data from sample RP109.

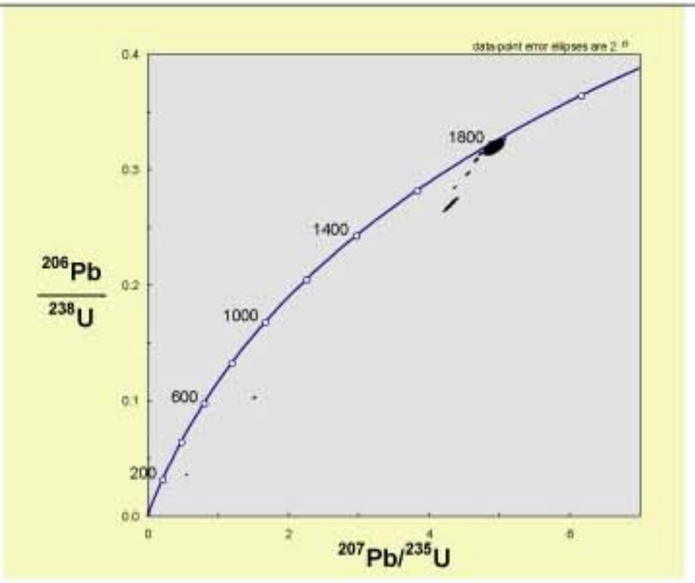

Figure DR-1 (f) Concordia diagram for all monazites and Z5 from sample RP109, with regression line for these 5 points shown for reference.